PROCEEDINGS, Thirty-Second Workshop on Geothermal Reservoir Engineering
Stanford University, Stanford, California, January 22-24, 2007
SGP-TR-183

IN SEARCH FOR THERMAL ANOMALIES IN THE COSO GEOTHERMAL FIELD (CALIFORNIA) USING REMOTE SENSING AND FIELD DATA

Mariana Eneva[1], Mark Coolbaugh[2], Steven C. Bjornstad[3], and Jim Combs[4]

[1]Imageair, Inc., 10513 Caminito Westchester, San Diego, CA, 92126
e-mail: meneva@imageair-inc.com
[2]Great Basin Center for Geothermal Energy, University of Nevada Reno, Reno, NV
[3]USN Geothermal Program Office, China Lake, CA
[4]Geo Hills Associates, Reno, NV

ABSTRACT

We attempt to identify thermal anomalies using thermal infrared (TIR) data collected over the Coso Geothermal Power Project with the spaceborne ASTER instrument. Our analysis emphasizes corrections for thermal artifacts in the satellite images caused by topography, albedo, and thermal inertia. This approach leads to noise reduction and has the potential to reveal thermal anomalies which are weak or not distinguishable in the uncorrected imagery. We have carried out field experiments concurrent with the collection of pairs of daytime and nighttime ASTER images over Coso. The field data include subsurface temperature measured with temperature probes at depths down to 1 m, surface temperatures recorded with a hand-held infrared camera and an infrared thermometer, reflectance of contrasting surfaces measured with a hand-held spectroradiometer for the purpose of estimating the albedo effect, and radiosonde atmospheric profiles of temperature, water vapor, and pressure in order to apply atmospheric corrections to the images. The combined use of remote sensing and field data is intended to evaluate the performance of remote sensing as a cost-effective geothermal exploration tool. We reason that if reliable thermal anomalies are identified at Coso, we can subsequently search for similar markers in TIR data collected over areas of unknown geothermal potential between Coso and Mono Lake in eastern California.

INTRODUCTION

Remote sensing can be used as a cost-effective tool to explore large areas for geothermal potential and subsequently select smaller targets for further exploration based on more expensive airborne and ground-based surveys. Useful applications include mineral mapping and identification of thermal anomalies associated with geothermal activity. These complementary techniques are best utilized together, because not all geothermal resources exhibit both elevated surface temperatures and mineral alteration. In this paper we report results from our search for thermal anomalies using images collected by the Advanced Spaceborne Thermal Emission and Reflection Radiometer (ASTER). For this purpose we use mainly thermal infrared (TIR) ASTER data products. The visible band is also used for correction of the albedo and topographic slope effects. At this stage we focus on the Coso Geothermal Power Project (Monastero, 2002) in the central part of eastern California. Our goal is to eventually extend our findings north-northwest, towards the Mammoth Geothermal Power Project, as the region between these existing geothermal fields is suspected to have significant geothermal resources. This is important in view of the increasing interest in electricity generation from renewable resources and, in particular, tapping into the potential 4,000 megawatts of additional power from geothermal energy in California (Sass and Priest, 2002).

Previous applications of optical and infrared remote sensing to geothermal fields have sought to characterize surface expressions of the underlying geothermal reservoirs (e.g., Kratt et al., 2006; Pickles et al., 2001; Martini et al., 2000). Closer to the type of application featured here, Calvin et al. (2002) used a daytime/nighttime pair of ASTER TIR scenes over the Brady Hot Springs geothermal area (Nevada) to identify a thermal anomaly associated with a nearby fault. Corrections for topographic slope orientation, albedo, and thermal inertia (Coolbaugh, 2003; Coolbaugh et al., 2007a) have been shown to increase the number of remotely sensed thermal anomalies by an order of magnitude compared with the TIR images without such corrections. High albedo is related to higher reflectance and less energy remaining for heating. Southern slopes receive more of the flux of solar irradiance than the northern slopes. Thermal inertia indicates how fast a material gets heated and cools off, and can be estimated from daytime/nighttime pairs of thermal satellite images.

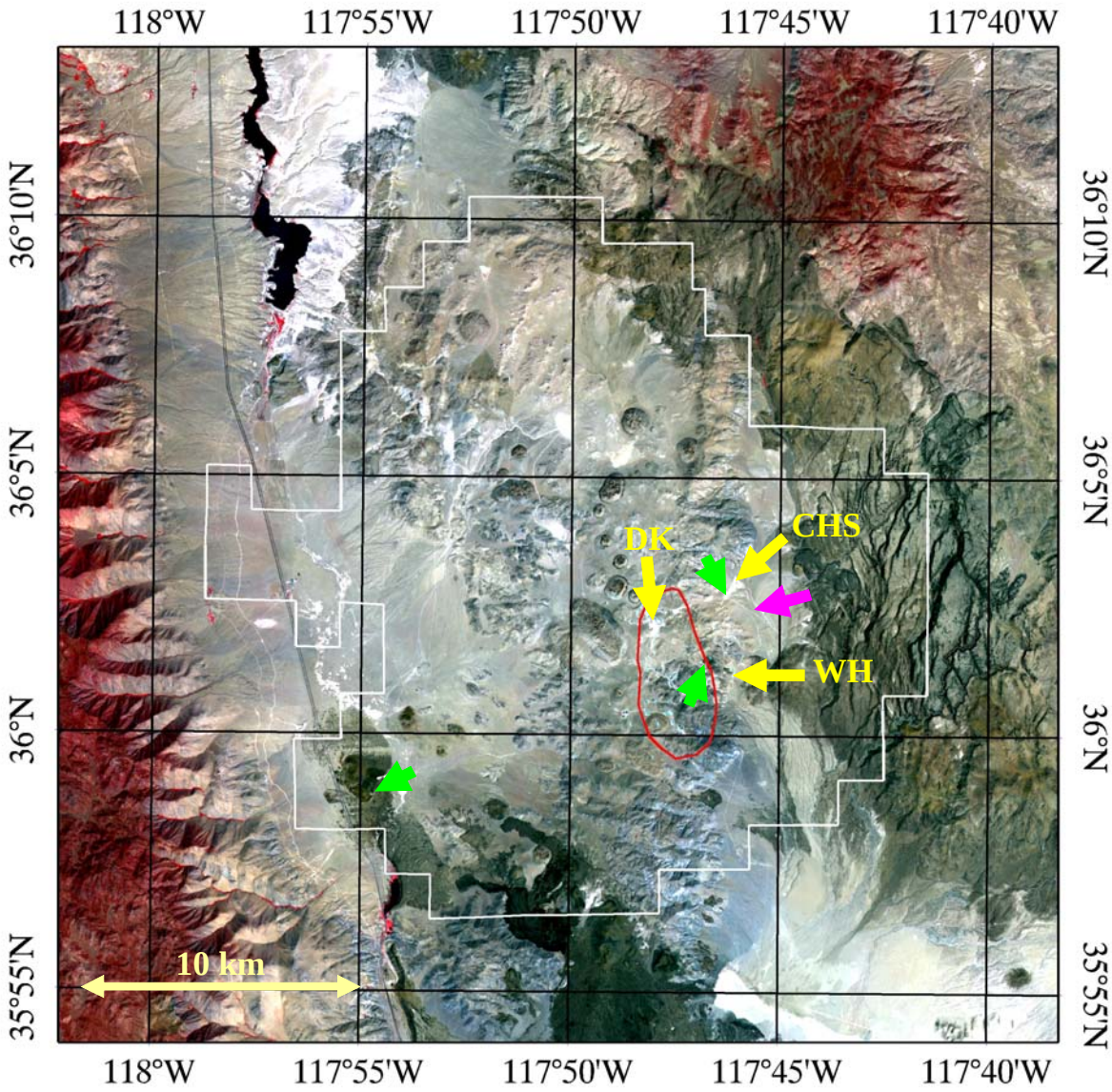

Figure 1. *ASTER coverage of the Coso KGRA (white polygon) extracted from two Level 1B VNIR images collected at 11:45 am (summer savings time) on August 22, 2006 (RGB: R=band 1, G=band 2, B=band 3). Production area is shown with a red outline. Yellow arrows point to locations of temperature probes along three lines in the Coso Hot Springs (CHS), Devil's Kitchen (DK), and Wheeler (WH) areas. Green arrows show locations of reflectance measurements. Magenta arrow points to the location where infrared thermometer was installed.*

Eneva et al. (2006) used Coolbaugh et al.'s (2007a) methodology to analyze a nighttime/daytime pair of ASTER TIR scenes collected over Coso in August 2001. This work also demonstrated that such corrections reduce noise and reveal thermal anomalies that are not seen in the uncorrected TIR scene. Missing in this analysis were field data that Coolbaugh et al. (2007a) showed to be important in the interpretation of remote sensing TIR imagery. For this reason, we organized a field experiment in July 2006 concurrent with the collection of a new daytime/nighttime ASTER pair over Coso. We collected subsurface and surface temperature data, reflection data for albedo estimates, and atmospheric profiles for correcting the imagery. However, clouds uncharacteristic for this time of the year in this area rendered the collected nighttime ASTER scene useless, while the quality of the daytime scene although better, was also questionable. For this reason, a second, significantly scaled-down field trip was organized in August 2006, when a good quality daytime/nighttime pair of ASTER scenes was collected concurrently with surface temperature and reflection measurements. Figure 1 shows part of the daytime scene; details are discussed below. Although weather and logistics reduced the usefulness of the field data we collected, we present

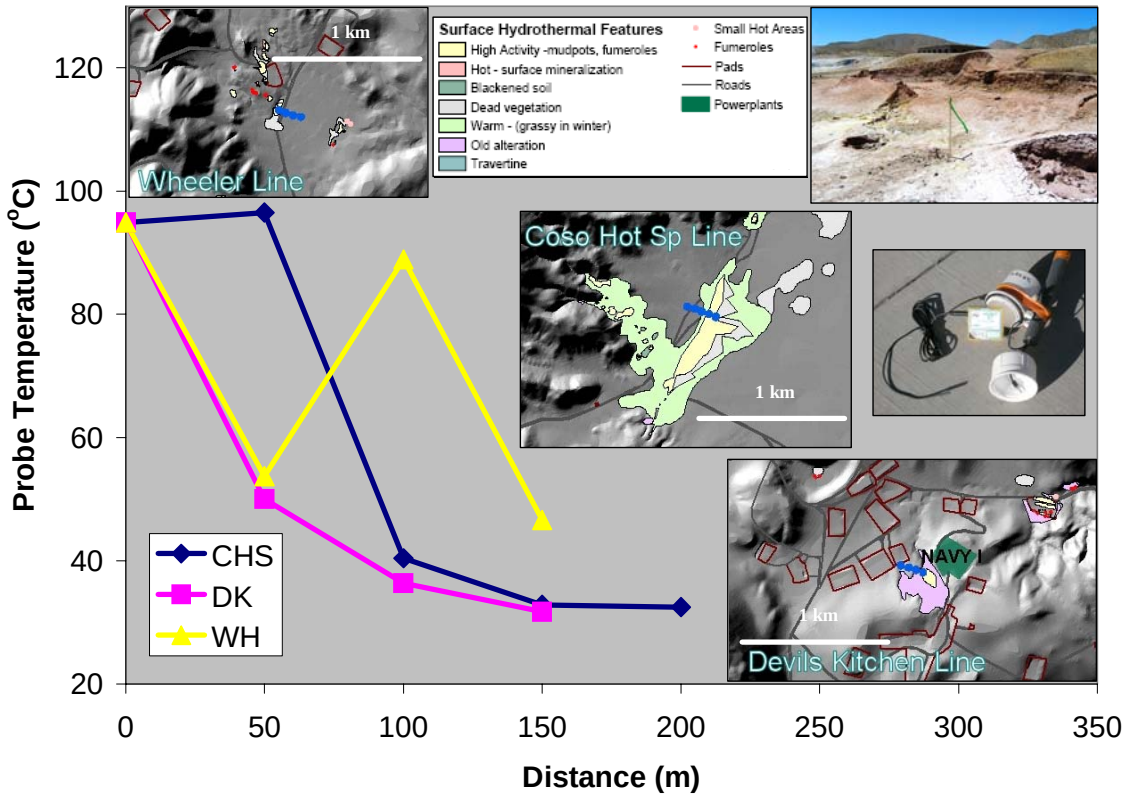

Figure 2. *Subsurface temperatures measured at 13 locations (blue circles in map insets) across hydrothermal features, as indicated. Distance is measured from the first probe along each line, starting within features and moving outwards. Photo insets show a probe and the surroundings of the CHS-2 probe. Map insets, with legend in middle top, courtesy of Bethiah Hall, USN GPO (China Lake, CA. Legend in bottom left is for temperature curves.*

them here as learning experience and in order to demonstrate what is possible in future work.

DATA

Satellite Thermal Infrared (TIR) Data

Compared with previous TIR remote sensing, ASTER is a unique instrument providing multispectral images in 14 different bands: (1) three visible and near-infrared (VNIR) channels (wavelengths 0.5 to 0.9 μm) at 15-m spatial resolution; (2) six short-wave infrared (SWIR) channels (1.6 to 2.43 μm) at 30-m resolution; and (3) five thermal infrared (TIR) channels (8 to 12 μm) at 90-m resolution. The most frequently used ASTER data product is Level 1B (radiance at sensor). Higher-level data products calculated from Level 1B include surface kinetic temperature (AST_08) and surface reflectance corrected for atmospheric effects (AST_07), both used in our work. The ASTER scenes are of size ~60-km X 60-km. The satellite passes every 16 days over a given site, although scenes are not necessarily collected with each passage. However, special scheduling makes it possible to collect a daytime/nighttime pair separated by a short time interval, ~36 hours for California.

We collected ASTER pairs in July and August, 2006, of which only the second pair could be used for our purposes. The nighttime image in the second pair was collected at 11 p.m. on August 20, and two adjacent daytime images were collected at 11:45 a.m. on August 22 (local, summer savings times). Figure 1 shows part of the mosaic built from the two daytime ASTER Level 1B VNIR images, covering the Coso known geothermal resources area (KGRA) and the current production area. Scenes were orthorectified using a USGS 30-m digital elevation model (DEM). Orthorectification is important in this case because the surface elevations in the Coso area vary rather significantly, from 720 m to 1550 m.

Field Data

Subsurface temperature measurements

Hobo XT temperature loggers (Figure 2) were used to record subsurface temperatures in 13 locations grouped along three lines across distinct hydrothermal features in the Coso Hot Springs (CHS), Devil's

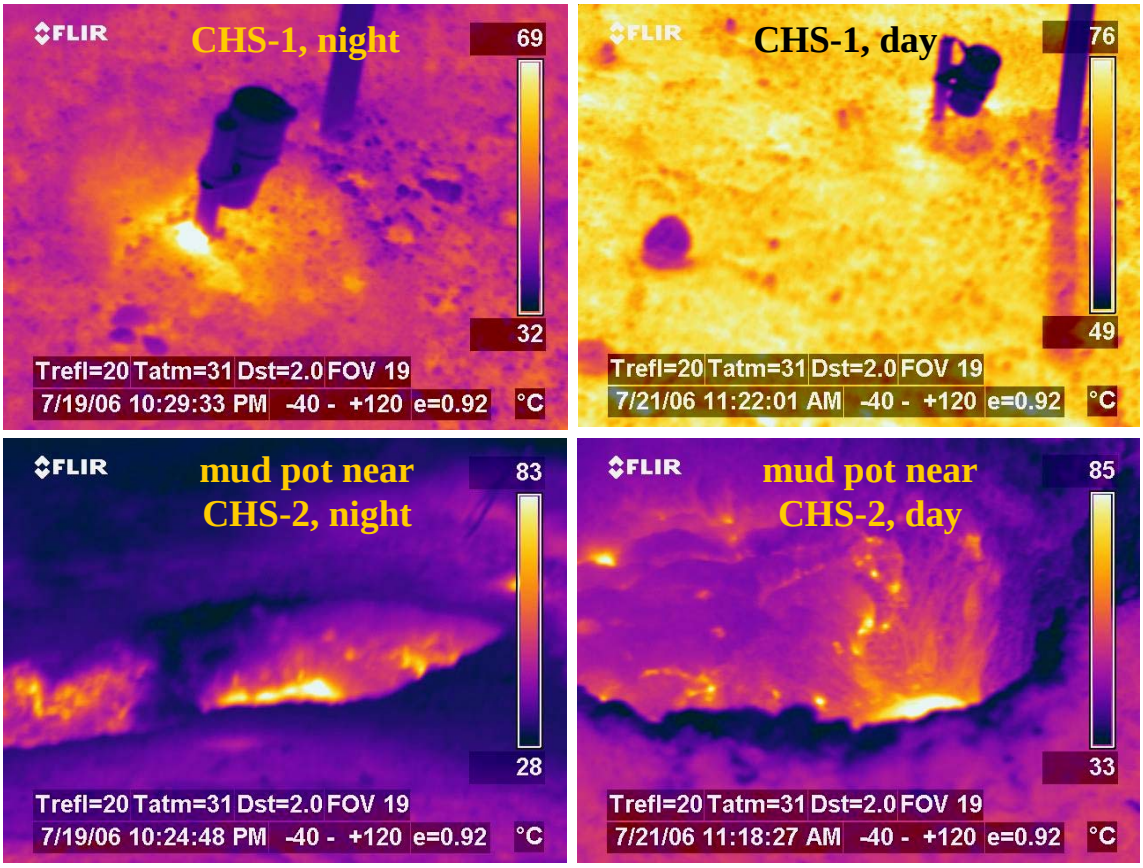

Figure 3. *Surface temperature measured with a hand-held FLIR-P65 infrared camera close to the times of satellite passages. Left – nighttime images; right – daytime images. Top – vicinity of the CHS-1 probe (probe and demarcation pole are cooler). Note hotter surface due to ground disturbance around probe. Bottom – mud pots near the CHS-2 probe.*

Kitchen (DK), and Wheeler (WH) areas. The locations of the three lines are marked with yellow arrows in Figure 1 and additional details are shown in Figure 2. The temperature probes were installed at depths 0.73 to 0.91 m (2.4 to 3 ft, as rock permitted). Probe locations were 50 m apart for each line. The recordings lasted about a week, including the times of satellite passages in July 2006. For any given site, subsurface temperatures remained rather constant. As could be expected, in each of the three groups, the temperatures decrease in the direction from the center of a hydrothermal feature towards its periphery.

Surface temperature measurements with a FLIR camera

We measured surface temperature around the times of satellite passages in July 2006 using a hand-held infrared camera FLIR P65. This was mostly done by collecting FLIR images at distances 2 to 3 m from the locations where the temperature probes were installed, as well as from a distance towards the surrounding rhyolite domes and hills. The idea was to make comparisons with the AST_08 scenes (kinetic surface temperature). Such a comparison is challenging enough due to the inevitable averaging over 90-m pixels in the satellite data, but in addition, the July ASTER data were too cloudy to use. Because of the expense to rent this equipment again, a FLIR camera was not used during the August field experiment. However, the FLIR images are still rather unique and it is instructional to examine the spatial distribution of surface temperature. Examples of the numerous images we collected are shown in Figure 3.

Surface temperature measurements with an infrared thermometer

An Omega OS534E infrared thermometer was installed in the area of the Coso Wash in August. It pointed at a point on bare soil. Temperatures were logged over a two day period. Figure 4 shows the diurnal changes of surface temperature, as well as images of the thermometer installation.

Reflectance measurements for albedo

In order to correct the AST_08 images for albedo, we collected reflectance data at 15 locations over surfaces of different color and texture, around the time of daytime satellite passage in August. For this pur-

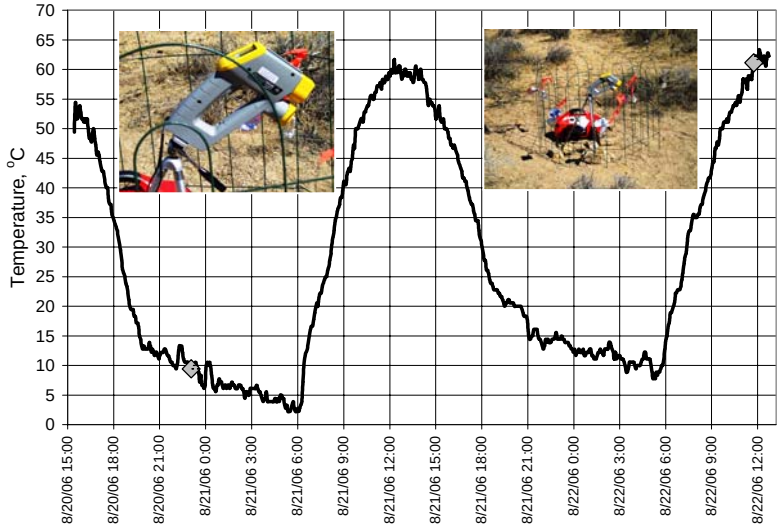

Figure 4. *Surface temperature measurements with an infrared thermometer over two days in August 2006. Grey diamonds indicate temperatures at the times of satellite passage. Insets show thermometer installation, with a portable power supply and a fence and ribbons to deter burros.*

pose we used a hand-held ASD FieldSpec spectroradiometer. The surfaces included bare soil, volcanic rock, red cinder, gravel, dirt road, and dry and live sage bush (Figure 5). These field data were used to evaluate coefficients in the relationship between the spaceborne reflectance data (AST_07) and a combination of albedo and topographic slopes, following the details described by Coolbaugh (2003) and Coolbaugh et al. (2007a).

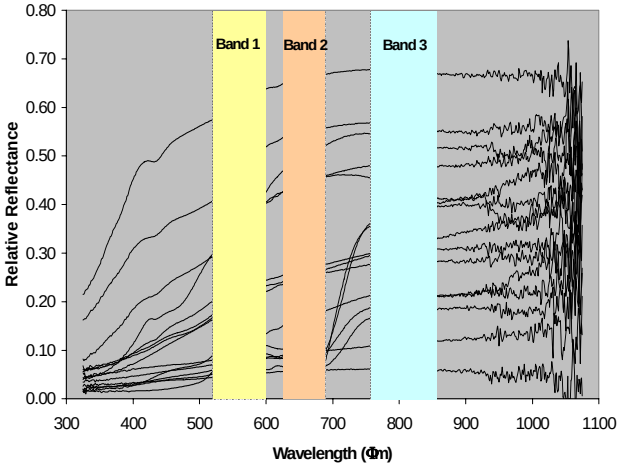

Figure 5. *Reflectance measured at various locations with a hand-held ASD FieldSpec spectroradiometer. Wavebands 1 to 3 correspond to ASTER VNIR. Dark to light surfaces are represented by increasing reflectance.*

Radiosonde atmospheric profiles

The AST_08 and AST_07 products incorporate a standard atmospheric correction. However, better correction is achieved if specific profiles of atmospheric temperature, water vapor, and pressure are available. We collected such data by launching radiosondes about half an hour before the two satellite passages in July. This was done with the assistance of the ASTER team at the Jet Propulsion Laboratory (JPL). Due to expense and logistic difficulties, radiosondes were not re-launched in August.

DATA ANALYSIS

A simplified heat energy model based on net surface radiation flux Q is used to correct for albedo and topographic slope, following the methodology described in detail by Coolbaugh (2003) and Coolbaugh et al. (2007a):

$$Q \sim (1\text{-}A)*M(Z)*cosZ' , \qquad (1)$$

where Q is the net radiation flux at the surface, A is the ground albedo, $cosZ'$ is the cosine of the angle between the surface normal and the sun's rays (calculated as so-called "shaded relief"), Z is the zenith angle, and $M(Z)$ is the atmospheric transmission depending on Z. The shaded relief can be calculated from the sun's elevation and declination for any given date and time of satellite passage. The albedo A is obtained as a weighted average from three band dependent albedo estimates A_w:

$$R_w = k_w*A_w*cosZ' + b_w \ , \qquad (2)$$

where R_w is taken from the AST_07 product (surface reflectance), $cosZ'$ is the same shaded relief as above, and the constants k_w and b_w are estimated from the field reflectance measurements as described by Coolbaugh (2003) and Coolbaugh et al. (2007a). These constants would have been 1 and 0, respectively, if it were possible to correct the AST_07 scene perfectly for atmospheric absorption and scattering effects. The subscript w indicates any of the three ASTER VNIR bands. In our case, we estimated k_w to be between 0.47 and 0.55 for the three bands, and b_w between 0.17 and 0.19.

The heat flux equation (1) is further integrated over time to model changes in the intensity of light and the position of the sun relative to the topographic slopes over the course of a day:

$$E \sim (1\text{-}A)*\sum\nolimits_t [M(Z)_t*cosZ'_t*D_t]*\Delta t_t , \qquad (3)$$

where E is the solar energy absorbed per unit area over the course of a day; Δt_t is the time interval for each component of the sum; D_t is a time decay factor ranging from 0 to 1, which is inversely proportional to the time gap between a given position of the sun and the time the imagery was acquired.

This simplified model accounts approximately for heat dissipation and is used to calculate pseudo-temperature images that are subtracted from the AST_08 (surface temperature) daytime and nighttime images. Both the daytime and the nighttime scenes are affected by differential heating during the day. This is particularly important to note for the nighttime images, because the Terra satellite passes only several hours after sunset.

The effect of thermal inertia is neutralized by summing the corrected daytime and nighttime AST_08 images, using weighing coefficients for the daytime and for the nighttime scenes, respectively. These weight factors are estimated from the images as described by Coolbaugh (2003).

This is a work in progress and we have currently completed the orthorectification of two Level 1B VNIR (no VNIR at night), three Level 1B TIR, and two AST_07 VNIR images. The orthorectification of the three AST_08 images has been most challenging and we are going through modifying previous processing steps. We have also completed the comparison of the AST_07 data with the field reflection data, which along with the shaded relief calculations has allowed us to estimate the coefficients in (2) above.

FUTURE WORK

The next steps in the work with the Coso data will be to perform the calculations in (3) and to remove the effect of thermal inertia. It is expected that this will assure noise reduction and that similar to our analysis of the August 2001 data (Eneva et al., 2006), some thermal features will be revealed that are not seen in the uncorrected AST_08 images. Further work will include reprocessing of the August 2001 data, as some steps were too simplified earlier, and comparing the results from 2001 and 2006 with each other and with topographic information from digital raster graphics (DRG) data available from the USGS.

We intend to arrange for future collections of nighttime/daytime ASTER pairs over the region north of Coso. These data will be analyzed with the methodology described here. We will strive to introduce improvements to some of the analysis steps and to take into account additional factors. Among those is vegetation, which does not represent a major problem for the Coso area, but we need to develop procedures for taking it into account in areas where it is more prominent. Furthermore, mineral alteration mapping not attempted so far in this area, could further increase the significance of remote sensing data as a cost-effective exploration tool. Although outside the scope of our current project, we plan on starting related analysis in near future. Finally, we intend to carry out more field studies at sites of interest, possibly using the rapid system of temperature measurements at 2-m depth described by Coolbaugh et al. (2007b).

CONCLUSIONS

ASTER TIR remote sensing data and various field measurements were recently collected in and over the Coso Geothermal Project in eastern California. A model is being applied to the TIR imagery that takes into account albedo, topographic and thermal inertia effects. Although simplified, this model is capable of eliminating false thermal anomalies and revealing thermal signals not seen in the uncorrected imagery. We expect to confirm and improve on earlier results (Eneva et al., 2006) from the analysis of ASTER data collected in the summer of 2001.

Due to unfavorable weather conditions, the ASTER images from July 2006 could not be used, and some of the field data we collected could not be utilized for comparison purposes as initially intended. However, the field data depict complementary aspects of the Coso geothermal field and are instructional in view of future applications.

ACKNOWLEDGMENTS

This project is funded by the California Energy Commission (CEC) and is partially matched by a NASA grant. Frank Monastero from the USN Geothermal Program Office (GPO) has made possible the logistics of collecting field data at Coso. Dave Meade and Chris Page from GPO helped with collecting the field data. Doug Stow and Pete Coulter from San Diego State University (SDSU) provided the ASD FieldSpec spectroradiometer and explained its use. Leon Maldonado from the Jet Propulsion Laboratory (JPL) has helped to make arrangements for the collection of the ASTER pairs. Mike Abrams and Elsa Abbott from JPL have been instrumental in the radiosonde launches.

REFERENCES

Calvin, W.M., M.F. Coolbaugh, and R.G. Vaughan (2002). "Geothermal site characterization using multi- and hyperspectral imagery." *Geothermal Resources Council Transactions*, **26**, 483-484.

Coolbaugh, M.F. (2003). "The Prediction and Detection of Geothermal Systems at Regional and Local Scales in Nevada using a Geographic Information System, Spatial Statistics, and Thermal Infrared Imagery." Ph.D. Thesis, University of Nevada Reno.

Coolbaugh, M.F., C. Kratt, A. Fallacaro, W.M. Calvin, and J.V. Taranik (2007a). "Detection of geothermal anomalies using Advanced Spaceborne Thermal Emission and Reflection Radiometer (ASTER) thermal infrared images at Brady's Hot Springs, Nevada, USA," *Remote Sensing of Environment*, in press.

Coolbaugh, M.F., C. Sladek, J.E. Faulds, R.E. Zehner, and G.L. Oppliger (2007b). "Use of rapid temperature measurements at 2-m depth to augment deeper temperature gradient drilling," In *Proceed. 32nd Workshop Geothermal Reservoir Engineering, Stanford University, January 22-24, 2007* (this issue).

Eneva, M., M.F. Coolbaugh, and J. Combs (2006). "Application of satellite thermal infrared imagery to geothermal exploration in east central California," *Geothermal Resources Council Transactions*, **30**, 407-411.

Kratt, C., M.F. Coolbaugh, and W.M. Calvin (2006). "Remote detection of Quaternary borate deposits with ASTER satellite imagery as a geothermal exploration tool," *Geothermal Resources Council Transactions*, **30**, 435-439.

Martini, B.A., E.A. Silver, D.C. Potts, and W.L. Pickles (2000). "Geological and geobotanical studies of Long Valley Caldera, CA, USA utilizing new 5-m hyperspectral imagery." In *Proceed. IEEE Int. Geoscience Remote Sensing Symposium, July 2000*.

Monastero, F.C. (2002). "Model for success: An overview of industry-military cooperation in the development of power operations at the Coso Geothermal Field in southern California." *Geothermal Resources Council Bulletin*, 188-194.

Pickles, W.L., P.W. Kasameyer, B.A. Martini, D.C. Potts, and E.A. Silver (2001). "Geobotanical remote sensing for geothermal exploration." *Geothermal Resources Council Transactions*, **25**, 307-312.

Sass, J., and S. Priest (2002). "Geothermal California: California claims the world's highest geothermal power output, with potential for even more production with advanced techniques." *Geothermal Resources Council Bulletin*, 183-187.